Hydrophobic Properties of New Epoxy-Silica Hybrids

Paola Cardiano

Dipartimento di Chimica Inorganica, Chimica Analitica e Chimica Fisica, University of Messina, Salita Sperone 31 S. Agata, 98166 Messina, Italy

Received 4 September 2007; accepted 10 January 2008
DOI 10.1002/app.27985
Published online 5 March 2008 in Wiley InterScience (www.interscience.wiley.com).

ABSTRACT: New products to be employed as coatings for construction materials have been synthesized. Room temperature blending of poly(bisphenolA-*co*-epichlorohydrin), glycidyl endcapped (DGEBA) and 3-aminopropyl-methyldiethoxysilane (AMTS), as well as of DGEBA, (3-glycidyloxypropyl)trimethoxysilane (GLYTS) and AMTS, in $CHCl_3$, employing different stoichiometric ratios, leads to transparent and crack free solids. The extent of epoxy cleavage during the hardening reaction and the hydrolysis of the $Si(OR)_x$ groups have been followed by ^{13}C NMR spectroscopy in solution; the solids have been characterized by means of Raman, FTIR, and TG-DTA studies. The hydrophobic properties of the resulting solids have been investigated by contact angle measurements on coated glass slides, and have been tailored by adding to the above mixtures two fluorine-containing comonomers, namely glycidyl-2,2,3,3,4,4,5,5,6,6,7,7,8,8,9,9-hexadecafluorononyl ether (GLY16F) and 3,3,3-trifluoropropyl-trimethoxysilane (TFP-TMS). Preliminary tests to evaluate the efficacy of the above products, as construction materials coatings, have been carried out by means of mercury intrusion porosimetry and water absorption by the wicking method. © 2008 Wiley Periodicals, Inc. J Appl Polym Sci 108: 3380–3387, 2008

Key words: coatings; hybrid materials; epoxy; fluorine comonomers

INTRODUCTION

The problems connected with ancient and modern construction materials outdoor exposition and its deleterious effects on architectural structures had led to the development of novel materials for stone conservation. These materials ought to consolidate already damaged structures and, at the same time, to protect the lithic substrates from further deterioration. The protective treatment goal is the protection of the ''skin'' of the stone, the thin stone layer were rainwater, gaseous pollutants, solid particulate, and thermal stress mainly exert their damaging effects. A protective agent must, above all, avoid the water penetration inside the stone as it is well established that water accounts for most of the degradation phenomena involving construction materials. Rainwater, on penetration inside a wall, is the vehicle of all the contaminants in the stone and, at the same time, may dissolve soluble salts and/or activate solid pollutants. Soluble salts crystallization is recognized as the most dangerous phenomenon since whenever supersaturation occurs inside the pores, the crystals, on growing, exert a pressure upon the pore walls that may lead to disruption.[1] As a consequence the main purpose of the protection of facades against water intrusion involves the coating of the stone surfaces with low surface energy materials. The use of silicon containing compounds and organic polymers to protect stone from the effects of decay is widespread even thought most of these materials have been previously marketed for industrial use rather than in the field of conservation of architectural structures.[2,3] Since these products are featured by some disadvantages, we turned our attention to the synthesis of epoxy-silica hybrids to be employed in stone coating.[4–6] Epoxy resins cured with aliphatic amines are extensively used as protective coatings for several applications[7] even though, in stone conservation, they do not match some fundamental requirements such as photostability or mechanical properties. The insertion of inorganic domains inside the organic network by means of a long-chain alkoxy-silane functionalized amine leads to a substantial modification of their chemical and physical properties. At the same time, the employment of fluorinated additives or comonomers ought to be very attractive since the presence of fluorine may give unique properties to the resulting material, such as enhanced hydrophobicity, chemical inertness, and weathering resistance.[8,9]

As a continuation of our previous work, we report here on the strengthening of pure poly(bisphenolA-*co*-epichlorohydrin), glycidyl endcapped (DGEBA) as well as of a mixture of DGEBA and (3-glycidyloxypropyl)trimethoxysilane (GLYTS) by means of the aliphatic aminosilane 3-aminopropyl-methyldiethoxysilane (AMTS) (Fig. 1). The ring opening reaction

Correspondence to: P. Cardiano (pcardiano@unime.it).

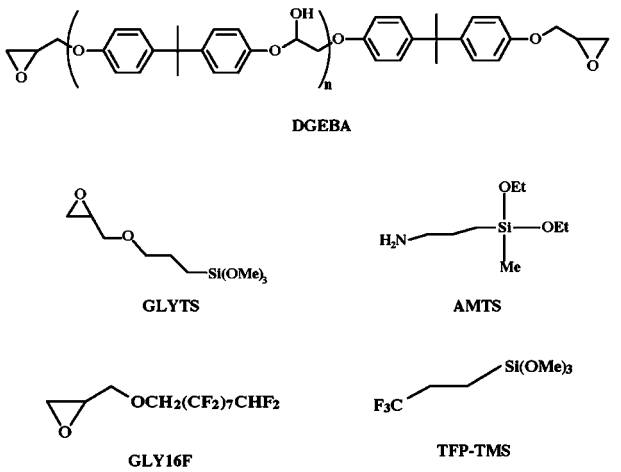

Figure 1 DGEBA, GLYTS, AMTS, GLY16F, and TFP-TMS.

has been monitored by means of solution ^{13}C NMR spectroscopy; the thermogravimetric, Raman and FTIR properties of the resulting solids are presented, together with their hydrophobic activity. Furthermore, in order to optimize the hydrophobic properties, two different fluorine-containing comonomers able to bind to the aforementioned epoxy resins, namely glycidyl-2,2,3,3,4,4,5,5,6,6,7,7,8,8,9,9-hexadecafluorononyl ether (GLY16F) and 3,3,3-trifluoropropyl-trimethoxysilane (TFP-TMS), have been added to the above blends and the consequent contact angle variations have been studied. GLY16F, bearing an epoxy ring, can easily undergo an oxirane cleavage by the amino group of AMTS, while TFP-TMS can interact with the active sites of AMTS and GLYTS, through hydrolysis and condensation of the alkoxy functional groups. In addition, porosity and water absorption properties were also investigated on a selected lithotype, properly treated with the aforementioned compounds, to preliminarily evaluate their efficacy as stone conservation materials.

EXPERIMENTAL

Poly(bisphenolA-*co*-epichlorohydrin), glycidyl end-capped (DGEBA) (Average M_n = 348 corresponding to an average degree of polymerization of 0.03; epoxy equivalent = 174), (3-glycidyloxypropyl)trimethoxysilane (GLYTS), 3-aminopropyl-methyldiethoxysilane (AMTS), glycidyl-2,2,3,3,4,4,5,5,6,6,7,7,8,8,9,9-hexadecafluorononyl ether (GLY16F), and 3,3,3-trifluoropropyl-trimethoxysilane (TFP-TMS) were purchased from SigmaAldrich and used as received. ^{13}C NMR spectra have been performed in $CDCl_3$ by means of a Bruker AMX R-300 spectrometer operating at 300.13 and 75.47 MHz, respectively. FTIR spectra have been obtained on Perkin-Elmer RX-I on KBr disks. Micro-Raman investigations have been performed on a 1000 Renishaw apparatus equipped with a cooled CCD detector and an Olympus microscope, using the 633 nm line of a He/Ne laser as excitation source and a laser power at the samples of 25 mW. Thermogravimetric analyses have been performed on Perkin-Elmer Pyris Diamond TG-DTA in the temperature range 25–800°C, under nitrogen or air atmosphere (50 mL/min) and heating rate of 10°C/min. In some cases, in order to gain a better resolution of the superimposed DTG signals, the measurements have been carried out also with a heating rate of 5°C/min but no significant improvements have been observed. As a consequence PeakFit 4 was employed to obtain the exact onset temperatures from DTG curves using a convoluted Gaussian signals profile.

Dynamic contact angle investigations have been performed on coated glass microscopy slides (26 × 76 × 1 mm^3 by Prestige) using the Wilhelmy method by means of KSV Sigma 700 tensiometer at the speed of 2 mm/min in Ultra Pure water (measured surface tension: 72.69 ± 0.06 mN/m). The glass slides were accurately cleaned by sulfuric acid/K-dichromate cleaning solution prior to use, then washed by ultrapure water and checked by measuring the surface tension of water. Then the slides were coated by dip coating method immersing the plates in the same solutions used for wicking experiments (see later) at a constant rate (20 mm/min) without delay time between immersions and withdrawn. After the dip coating cycles, the coated slides were aged for 30 days at 50°C and then contact angle measurements have been performed. The discussed contact angles correspond to the average of the measurements carried out on five glass slides treated in the same way. Furthermore, in order to show the wetting effect of water on the samples' surfaces, five continuous immersion/withdrawn cycles have been performed on each coated specimen, but no significant variation in the contact angle has been detected.

The conservation experiments were performed on samples of a selected lithotype, the Comiso calcarenite (COM), that were allowed to adsorb the conservation mixtures by capillarity (6 h) and by total immersion (24 h). The treated samples were then cured for 2 months at 30°C and 50% RH. Each experiment was performed on five sets of regular samples of 1 × 0.5 × 3 cm^3 carefully washed with deionized water and dried at 60°C up to constant weight. Mercury porosimetry experiments have been carried out by means of low-pressure (400 kPa) and high-pressure (200 MPa) Fisons Instruments Pascal porosimeters following the Normal recommendations[10] on stone samples treated with 10 wt % chloroform solutions of DGEBA/AMTS in 1 : 1 (**1**), 1 : 2 (**2**), as well as on DGEBA/GLYTS/AMTS in 1 : 1 : 1.5 (**3**) and 1 : 1 : 2.5 (**4**) stoichiometric ratios. The water absorption tests by the wicking method were performed on

lithic samples treated with the solutions **1** and **3** as well as on **1** and **3** added of the fluorine comonomers GLY16F and TFP-TMS at 10 wt %, where the fluorine-containing species weight percentage (wt %) is referred to DGEBA.

Once the treated samples were cured as above, the capillarity water absorption was performed by wicking method suspending the lithic samples to the hook of a Wilhelmy balance. Moving down the hook one of the lithic sides was kept in contact with water surface.[11] The lateral sides of the cubic samples were covered with silicone to hinder the water absorption along the perimeter and to obtain capillarity rise only by the proper side. The mass variation of the samples has been automatically recorded by a computer, as a function of time.

RESULTS AND DISCUSSION

DGEBA and GLYTS, being characterized by the presence of oxirane groups, may undergo epoxy opening when reacted with AMTS, leading to the formation of secondary and/or tertiary amines. At the same time both GLYTS and AMTS may crosslink via hydrolysis and condensation of alkoxysilane fragments forming species containing Si—O—Si moieties under the basic conditions provided by AMTS.

Room temperature reaction between 3 mmol of DGEBA dissolved in 10 mL of $CHCl_3$, in an open vessel, and AMTS in 1 : 1 (**1**) and 1 : 2 (**2**) ratios, leads, after less than 24 h, to the formation of rubbery and transparent solids, suggesting that in these experimental conditions the $Si(OR)_2$ hydrolysis reaction is kinetically preferred. On the contrary, whenever the above reactions are carried out in a vessel sealed with parafilm, the hydrolysis is slower. In fact, if the blends are allowed to absorb slowly water from air moisture, they keep liquid longer with the formation of glassy and crack-free solids after 20 and 15 days, respectively, depending on the epoxy/amine ratio employed. As far as ternary blends are concerned, when 3 mmol of DGEBA dissolved in 10 mL of $CHCl_3$ are allowed to react, in an open system, with GLYTS and AMTS in 1/1/1.5 (epoxy equivalent/amine hydrogen equivalent 1/1) (**3**) and 1/1/2.5 (**4**) ratios, respectively, the reaction follows a similar trend: once again it is slower when performed in a closed vessel while following the same experimental conditions as before, a macroscopical increase in the viscosity can be observed until the formation of transparent and crack-free solids occurring in 20 and 17 days, respectively, depending on the amount of AMTS in the mixture. All the above solids have been cured at 45°C for 30 days prior to characterization.

The evolution of epoxy ring cleavage as well as the hydrolysis of the $Si(OR)_x$ groups has been followed by j-mod pulse sequence ^{13}C NMR in $CDCl_3$ solution. As far as **1** blend (epoxy equivalent/amine hydrogen equivalent 1/1) is concerned, the collected spectra show, after two days, the appearance of the propylic CH_2 resonances accounting for the formation of a secondary amine (51.74, 23.28, and 11.23 ppm) together with the resonances arising from oxirane opening reaction, namely the CH_2 at 52.62 ppm and the CH, in the inverted region of the spectra, at 68.11 ppm. At the same time the spectra experience the progressive disappearing of the peaks of the α carbon to NH_2 group of AMTS (44.95 ppm) as well as of the resonances centered at 44.55 and 50.00 ppm attributable to CH_2 and CH belonging to the epoxy ring, respectively. After 7 days, signals due to tertiary amines start to grow at 58.00, 20.07, and 11.12 ppm suggesting the involvement of the formed secondary amine in epoxy ring opening reaction; after 14 days the starting compounds resonances are hardly detectable indicating a nearly complete involvement of DGEBA and AMTS reactive groups in the reaction. Furthermore, at a later stage of the reaction the resonances due to the other reactive fragment of AMTS, namely $Si(OCH_2CH_3)_2$, at 58.19 and 18.30 ppm, respectively, start to decrease and the spectra experience the appearance of new nearby peaks attributable to partially hydrolyzed $Si(OC_2H_5)_{2-x}(OH)_x$ (x = 1,2) groups. In addition, the band at −5.05 ppm, due to methyl bound to silicon of AMTS and the aromatic signals of DGEBA start to decrease so that new nearby peaks appear as well.

As expected, the spectra of **2** shows, after 7 days, beside the signals due to unreacted AMTS, the complete disappearance of epoxy resonances. Again, **2** spectra display new resonances accounting for the hydrolysis reaction beginning.

Addition of GLYTS to the blend **1** slightly influences the course of the reaction. Solution ^{13}C NMR spectra of **3** show the peaks due to the DGEBA epoxy opening after 2 days while the signals at 51.66 and 67.78 ppm, attributable to GLYTS epoxy cleavage, are detectable only after 6 days suggesting a lower reactivity of aforementioned oxirane group with respect to DGEBA one. After 16 days, the CH resonance due to GLYTS epoxy ring is still well detectable suggesting the incomplete involvement of GLYTS in the reaction while the DGEBA oxirane peaks are no more visible. The $Si(OCH_3)_3$ groups undergo faster hydrolysis reaction than $Si(OEt)_2$ ones; in particular, the inverted methoxy signal at ca. 50 ppm starts to gradually decrease before the ethoxy ones, being replaced by other peaks falling in the same range. The spectra collected for **4** displays, after 14 days, the primary amine signals at 44.95, 27.17, and 10.88 ppm accounting for AMTS in excess.

The whole of collected NMR data suggests that (i) epoxy cleavage is the prominent reaction while hydrolysis occurs at a lower rate, (ii) DGEBA epoxy ring starts to react before GLYTS one and (iii) $Si(OCH_3)$ undergo faster hydrolysis with respect to $Si(OCH_2CH_3)$.[12]

Addition of the fluorine-containing comonomers GLY16F and TFP-TMS to **1–4** blends (in a low percentage due to their scarce solubility in chloroform) does not change the macroscopic evolution of the reactions. Various attempts to follow their characteristic resonances by means of solution NMR have been performed, but, as expected, being too low their amount in the blends, no clear results have been obtained. Nevertheless, the presence of fluorine in the bulk of the solids was confirmed by means of elemental analysis whose results are compatible with its theoretical amount [fluorine content found by elemental analysis: 3.57% (**1**+GLY16F); 1.39% (**1**+TFP-TMS); 2.56% (**3**+GLY16F); 1.03% (**3**+TFP-TMS)]; various attempts to detect the C—F stretching signal by FTIR gave no clear results due to the presence of the broad absorption of Si—O—Si moiety in the same range of the spectrum.

As far as Micro Raman investigations on solid samples are concerned, in the region 1200–1300 cm^{-1}, where the peaks accounting for the epoxy inplane expansions and contractions are visible, **3** is the only product that shows a signal. This experimental evidence confirms what already observed by means of solution NMR spectroscopy for **3** blend. Furthermore, as the spectra of **1–4** do not show the band of $Si(OCH_2CH_3)_2$ of AMTS at 639 cm^{-1} and the $Si(OCH_3)_3$ peak of GLYTS at 648 cm^{-1} is not visible anymore in **3** and **4**, the absence of unhydrolyzed alkoxy groups in all the investigated solids can be suggested. Unfortunately, since DGEBA is featured by some bands in the range 400–500 cm^{-1}, the formation of the Si—O—Si network cannot be unequivocally confirmed from Raman investigations. As a consequence FTIR investigations on solid samples have been carried out. From the collected spectra, the only valuable information is the broad absorption between 1000 and 1200 cm^{-1}, culminating at 1023 and 1080 cm^{-1}, due to Si—O—Si stretching vibrations. The presence of various medium intensity bands in the 900–980 cm^{-1} range in all the studied spectra did not allow making speculations about the presence of residual unreacted silanole groups.

To investigate the thermal stability of the polymers, thermogravimetric scannings have been carried out both in dynamic nitrogen and air atmosphere. Tables I and II report the temperatures of onset and maximum volatilization, the corresponding rates together with the mass losses for each process. The **1–2** mixtures heat treatment under nitrogen flow (Table I) show a common trend with (1) the first decomposition step featured by a T_{max} at 361 and 387°C for **1** and **2** respectively; (2) a main endothermic degradation stage at $\sim$ 430°C corresponding to the polymer degradation temperature; (3) a high temperature decomposition process culminating at $T_{max} \sim 515$°C. As a common feature all the products also show a low-temperature step at about 130°C (not reported in the table) attributed to the evolution of water, residual solvents, and condensation products formed during the ageing of the polymers or produced during the networking induced by the thermal treatment. The rate of mass loss for the last thermal event as well as the residual mass at 800°C are found to be dependent on the amount of DGEBA. In particular, by increasing DGEBA in the mixture, the rate of the above event is lower and the residual mass at 800°C decreases as follows **2** > **1**. As can be inferred from Table I, addition of GLYTS to the mixture **1** increases the thermal stability of the resulting blend as for **3** the first degradation event

TABLE I
Thermogravimetric Results Obtained for 1–4 Blends in the Temperature Range of 25–800°C, Under Nitrogen Flow (50 mL/min)

	1	2	3	4
Residual mass Res. 200°C (%)	92.9	92.8	96.8	92.8
First event				
T_{init} (°C)	319	334	344	324
T_{max} (°C)	361 (2.19%/min)	387 (3.47%/min)	426 (5.31%/min)	422 (4.36/min)
ΔM (%)	15.3	16.0	51.7	45.0
Second event				
T_{init} (°C)	348	344	415	408
T_{max} (°C)	432 (7.04%/min)	430 (4.83%/min)	502 (1.79%/min)	495 (2.18%/min)
ΔM (%)	42.2	33.0	15.9	18.2
Third event				
T_{init} (°C)	445	430		
T_{max} (°C)	517 (1.64%/min)	510 (2.25%/min)		
ΔM (%)	13.5	20.3		
Residual mass Res. 800°C (%)	21.9	23.5	29.2	29.6

TABLE II
Thermogravimetric Results Obtained for 1–4 Blends in the Temperature Range of 25–800°C, Under Air Flow (50 mL/min)

	1	2	3	4
Residual mass Res. 200°C (%)	91.1	92.3	96.4	92.2
First event				
T_{init} (°C)	217	229	195	203
T_{max} (°C)	281 (3.15%/min)	274 (1.99%/min)	268 (2.90%/min)	272 (1.99%/min)
ΔM (%)	16.6	10.3	19.0	9.6
Second event				
T_{init} (°C)	268	260	240	258
T_{max} (°C)	339 (2.09%/min)	348 (2.07%/min)	341 (1.93%/min)	348 (2.04%/min)
ΔM (%)	14.7	17.8	15.1	20.4
Third event				
T_{init} (°C)	327	302	247	251
T_{max} (°C)	404 (1.65%/min)	398 (1.67%/min)	403 (1.75%/min)	402 (1.68%/min)
ΔM (%)	10.1	7.6	12.3	6.0
Fourth event				
T_{init} (°C)	331	361	420	415
T_{max} (°C)	434 (1.59%/min)	457 (1.51%/min)	525 (1.38%/min)	527 (1.35%/min)
ΔM (%)	4.1	9.0	4.5	8.1
Fifth event				
T_{init} (°C)	413	418	475	480
T_{max} (°C)	541 (2.56%/min)	553 (2.16%/min)	575 (1.95%/min)	582 (1.86%/min)
ΔM (%)	32.2	26.7	24.7	23.1
Residual mass Res. 800°C (%)	13.4	20.9	20.8	25.0

starts ~ 25°C higher than **1**, while **2** and **4** begin to decompose in a comparable temperature range. Furthermore, for **3** and **4** the residual masses at 800°C is much higher than those observed for GLYTS-free blends suggesting that the presence of GLYTS has an important bearing on the degradation behavior of the products at high temperatures, probably due to the increased amount of silica in the solids. In addition, for **3** and **4** blends, the aforementioned first decomposition step occurring in the range 420–430°C represents also the main decomposition event, namely the polymer degradation temperature, with high corresponding mass losses. For these blends another decomposition event, endothermic in nature, at about 500°C can be observed. It is worth to mention that to achieve information about T_{onset} of every thermal process, being the thermograms featured by overimposed steps, the signals fitting and deconvolution have been carried out (Fig. 2).

The heating of the **1–2** blends in oxidative environment leads to different mass residuals at 800°C; by increasing AMTS in the blends, the residuals are slightly different than the theoretical amount of silica (Table II). The thermo-oxidative behavior of the above solids is complex being characterized by five steps, ranging from T_{max} of ~ 270–550°C. As a consequence, the fitting and deconvolution of the three DTG curves in the temperature range 100–800°C have been carried out. Even thought in the discussed tables only the observed signals have been reported, this procedure allows to detect other hidden processes hardly recoverable from the experimental data. The oxidative heating of **3** and **4** shows a complex combustion behavior as well; the higher T_{max} featuring the last two events as well as the higher re-

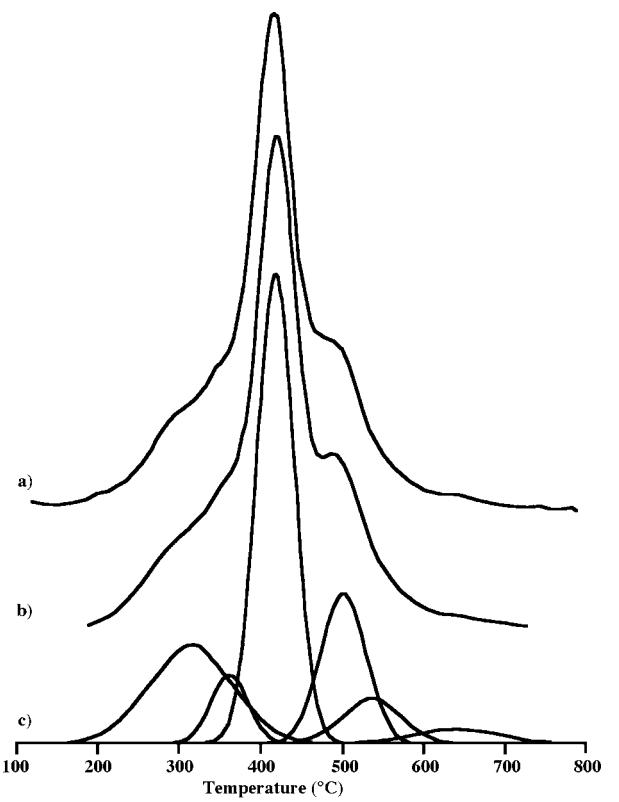

Figure 2 DTG curve of sample **3** under nitrogen flow (a) global (b) and single peak (c) fitting curves obtained with PeakFit.

sidual mass at 800°C with respect to **1** and **2**, suggest a higher complexity of the resulting network. For **3** and **4** the process at $T_{max} \sim 400$°C cannot be confidently detected from the experimental signal so that the fitting and deconvolution of the curves have been performed as well (Fig. 3). As can be inferred from Table II, the ratio of weight losses as well as the corresponding rates (except the higher temperature process) are found to be dependent on the amount of AMTS suggesting that though similar, the extent of the chemical reactions occurring during heating is influenced by the ceramic content. TG-DTA investigations have been carried out also on fluorine-containing solids, but, as expected due to the low amount of fluorine comonomers in the blends, the scannings appear very similar to those obtained for fluorine-free solids.

Hydrophobic properties

Lithic materials, natural or artificial, are usually featured by a very high wettability because of the presence on the stone surface of hydrophilic fragments such as hydroxyl or carbonate. The most used approach to hinder water penetration inside lithic substrates consists in the impregnation of the stone with hydrophobic materials able to lower the surface energy of the lithotype, once coated.[13] Bearing this

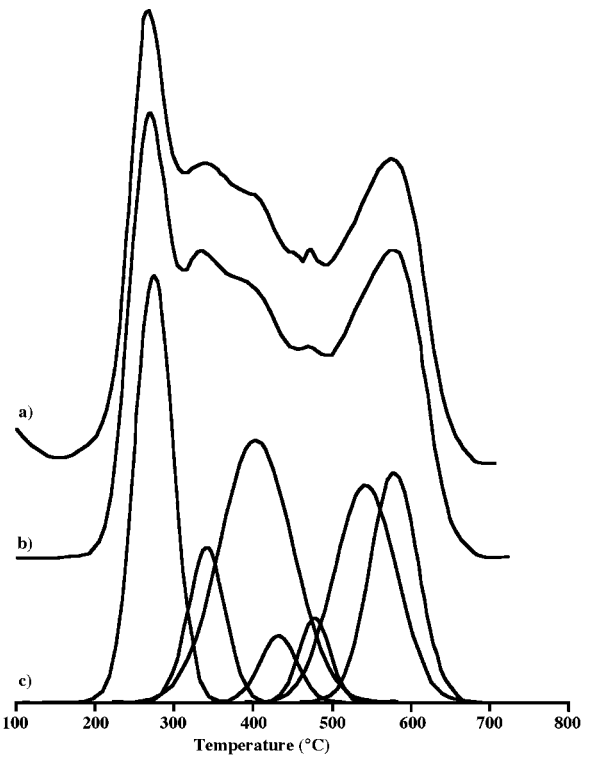

Figure 3 DTG curve of sample **3** under air flow (a) global (b) and single peak (c) fitting curves obtained with PeakFit.

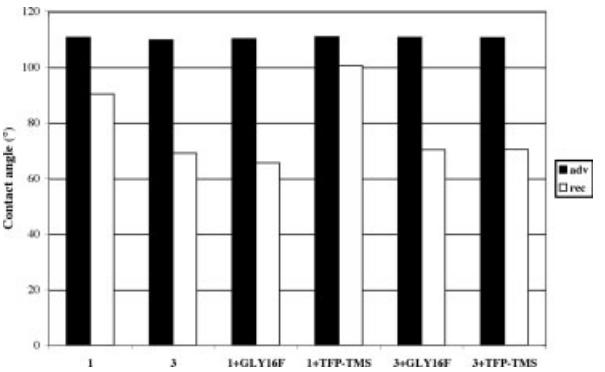

Figure 4 Dinamic contact angles measured by Wilhelmy method on coated glass slides.

in mind the hydrophobic properties and hence wettability of **1–4** have been investigated by means of dynamic contact angles measurements, where the advancing contact angle (θ_{adv}) accounts for the most hydrophilic portion of the surface while the receding contact angle (θ_{rec}) quantitatively represents the most hydrophobic. The experiments were carried out either on glass slides as on stone samples properly treated with the above mixtures, being the results of the last experiments not reliable (results not reported), very likely due to enhanced surface roughness and heterogeneity. As preliminary measurements on glass slides showed that hydrophobic behavior of **1–2** and **3–4** is very similar, we selected two representative blends, namely **1** and **3** to perform further investigations. The modification of the surface properties of **1** and **3**, following the addition of two fluorine-containing comonomers, namely the long-chained fluorinated epoxy glycidyl-2, 2,3,3,4,4,5,5,6,6,7,7,8,8,9,9-hexadecafluorononyl ether (GLY16F) and the fluorinated silane 3,3,3-trifluoropropyl-trimethoxysilane (TFP-TMS) was also investigated. The glasses coated with **1** mixture, without any fluorine additive, show remarkable hydrophobic properties being featured by very high values for the advancing ($\theta_{adv} = 110°$) and receding ($\theta_{rec} = 90°$) contact angles. It is to underline that the receding contact angle of an ideal hydrophobic agent should not be less than 90°. The addition of the two fluorinated species has an opposite effect on the hydrorepellent properties of **1** and **3**: while TFP-TMS induces a significative increase of the receding angle ($\theta_{rec} = 100°$) leaving mostly unchanged the advancing one (Figs. 4 and 5), for the mixture containing GLY16F a marked worsening of the receding angle ($\theta_{rec} = 66°$) was observed so that the difference between the two angles reaches the highest value. Although fluorinated materials are featured by very low surface energy, the relationship high fluorine content versus high contact angle is not straightforward as it depends, inter alias, on the structure net-

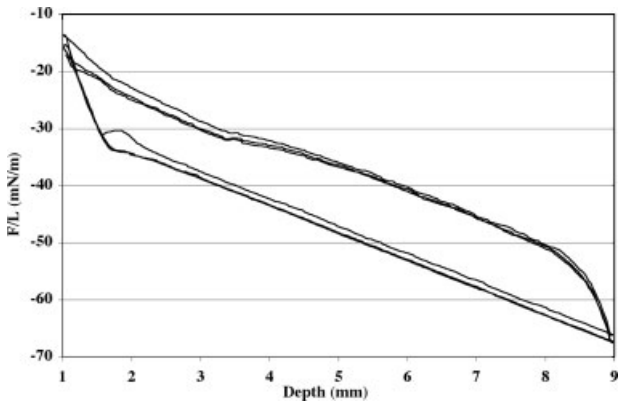

Figure 5 Force versus Immersion Depth hysteresis diagram for **1+TFP-TMS**.

work, segregation and assembly of the fluorinated segments at the interface air/polymer. It would appear that the long fluorinated chains of GLY16F are able to shield the water from the polar lithic backbone but, at the same time, the segregation of the fluorinated fragments is such to induce the formation of hydrophilic domains with higher surface energy. Species **3** provides materials that are as hydrophobic as those obtained by adding the fluorinated species GLY16F and TFP-TMS. Both advancing and receding contact angles measured on **3** coated glasses are in fact independent from the presence of fluorine-additives in the blends with values (θ_{adv} = 110° and θ_{rec} = 70°) mostly unchanged; as a consequence, it seems that in these blends the hydrophobic properties are mainly imparted by the parent network rather than by the fluorinated fragments on the surface.

To understand if the discussed blends may represent also a good barrier against water penetration into the stone, capillary absorption tests by the wicking method directly on lithic samples have been carried out. Figure 6 displays the capillarity behavior of coated COM samples compared with the

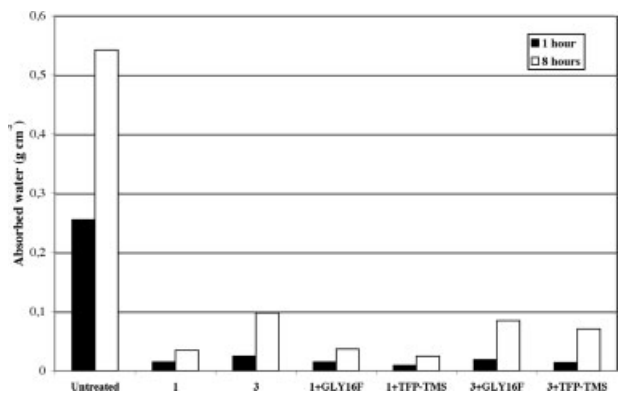

Figure 6 Capillarity water absorption measured by wicking method on COM treated samples.

TABLE III
COM Porosimetric Data

	untr	1	2	3	4
Total porosity (%)	19.1	13.8	13.4	13.9	13.1
Bulk density (g cm^{-3})	2.33	2.24	2.27	2.31	2.28
Average pore radius (μm)	0.21	0.14	0.12	0.18	0.16
Pore radius ranges (μm)		Relative volume (%)			
>5	5.11	0.75	0.39	1.06	1.37
5–2	3.65	0	0	0	0
2–1	0.36	0	0	0	0.11
1–0.5	1.09	0.11	0.1	0	0
0.5–0.4	1.09	0	0.1	0	0
0.4–0.3	4.38	0.35	0.1	0.11	0.21
0.3–0.2	32.12	7.55	3.02	6.05	6.86
0.2–0.1	27.55	74.3	77.39	79.61	74.76
0.1–0.05	10.22	9.32	10.14	8.6	9.29
0.05–0.025	4.38	3.78	4.29	3.5	4.01
0.025–0	10.04	3.71	4.48	1.27	3.38

uncoated stone, after 1 and 8 h. Independently from the mixture employed, DGEBA/AMTS coatings are able to considerably reduce the amount of absorbed water both at the beginning of the test and at saturation. In particular, the blend **1** added of TFP-TMS represents the best candidate to suppress water intrusion inside the stone. The water absorption suppression induced by **3** mixtures is slightly lower; nevertheless it is still very high. Furthermore, among the **3** mixtures, the one added with TFP-TMS represents the most effective waterproofing coating.

It is well known that the capillarity properties of a porous structure are mainly conditioned by the size of the pores and, as a consequence, by stone pore size distribution. As micropores are the main responsible for capillary rise phenomena, one of the prerequisites that must be fulfilled in a conservation treatment is the decrease of the total porosity without the shifting of the voids towards smallest pores.

In order to test the alterations induced in the pore network of the stone by the protective treatments, the stone samples, properly treated with the above mixtures, were investigated by mercury intrusion porosimetry which gives information on the total porosity, average pore radius and pore size distribution (Table III). The treatment of COM with the conserving mixtures **1–4** induces a decrease either in the total porosity as in the average pore radius. In particular the most effective blends, **2** and **4**, namely the ones richer in AMTS, lead at least to a 30% decrease of voids with respect to the untreated stone. The treatments of the COM stone with the **1–4** mixtures, as described in the Experimental Section, induce similar effect on the pore size distribution of all the stone samples. The treated samples experience the partial filling of the pores ranging from 0.2 to 100 μm as well as of the micropores leaving mostly unchanged the pores having a radius between 0.0025

and 0.1 μm. As a consequence, the pore size distribution after the conservation treatment appears mainly concentrated in the range 0.1–0.2 μm.

CONCLUSIONS

The reaction of the aminosilane AMTS with the epoxy DGEBA or with DGEBA and GLYTS mixtures lead to visually transparent, crack-free and insoluble solids. The reactions, under controlled experimental conditions, proceeds stepwise: polymerization of the epoxy groups on the organic side followed by hydrolysis and condensation of the $Si(OR)_x$ groups on the inorganic side to form Si—O—Si inorganic domains as detected by FTIR spectra. The TG-DTA investigations of the solids display a common trend mainly conditioned by the reaction stoichiometry thus reflecting the ceramic content as well as differences in the complexity of the formed structures, being the GLYTS-containing products featured by a higher stability both in nitrogen and air atmosphere. The hydrophobic properties of the above solids have been tailored by adding to the reaction mixtures two fluorine-containing comonomers, namely GLYTS16F and TFP-TMS. The very high hydrophobic activity featuring **3** is poorly enhanced by the presence of fluorine-additives, both on glass slides and on lithic samples. The performances displayed by **1** are very good as well, nevertheless the addition of TFP-TMS dramatically improves the measured contact angles; this behavior is fully confirmed by wicking experiments so that **1** mixture with TFP-TMS represent the most effective barrier, among the selected blends, able to impart strong hydrophobicity to the coated surface.

References

1. Scherer, G. W. Cem Concr Res 1999, 29, 1347.
2. Cocca, M.; D'Arienzo, L.; Gentile, G.; Martuscelli, E.; D'Orazio, L. New Polym Mater ACS Symp Ser 2005, 916, 370.
3. Mosquera, M. J.; De Los Santos, D. M.; Montes, A. Mater Res Soc Symp Proc 2005, 852, 81.
4. Cardiano, P.; Sergi, S.; Lazzari, M.; Piraino, P. Polymer 2002, 43, 6635.
5. Cardiano, P.; Mineo, P.; Sergi, S.; Ponterio, R. C.; Triscari, M.; Piraino, P. Polymer 2003, 44, 4435.
6. Cardiano, P.; Ponterio, R. C.; Sergi, S.; Lo Schiavo, S.; Piraino, P. Polymer 2005, 46 1857.
7. Ellis, B. Chemistry and Technology of Epoxy Resins; Chapman & Hall: London, 1998.
8. Walters, K.B.; Schwark, D. W.; Hirt, D. E. Langmuir 2003, 19, 5851.
9. Jeong, H. J.; Kim, D. K.; Lee, S. B.; Kwon, S. H.; Kadono, K. J Colloid Interface Sci 2001, 235, 130.
10. Normal Protocol 4/80. Distribuzione Dei Pori in Funzione Del Loro Diametro; CNR-ICR: Rome, 1980.
11. Brugnara, M.; De Gasperi, E.; Della Volpe, C.; Maniglio, D.; Penati, A.; Siboni, S.; Toniolo, L.; Poli, I.; Invernizzi, S.; Castelvetro, V. Colloid Surf A 2004, 241, 299.
12. Hench, L. L.; West, J. K. Chem Rev 1990, 90, 33.
13. Alvarez de Buergo Ballester, M.; Fort Gonzàlez, R. Prog Org Coat 2001, 43, 258.